Supporting Information

Courtemanche et al. 10.1073/pnas.1308257110

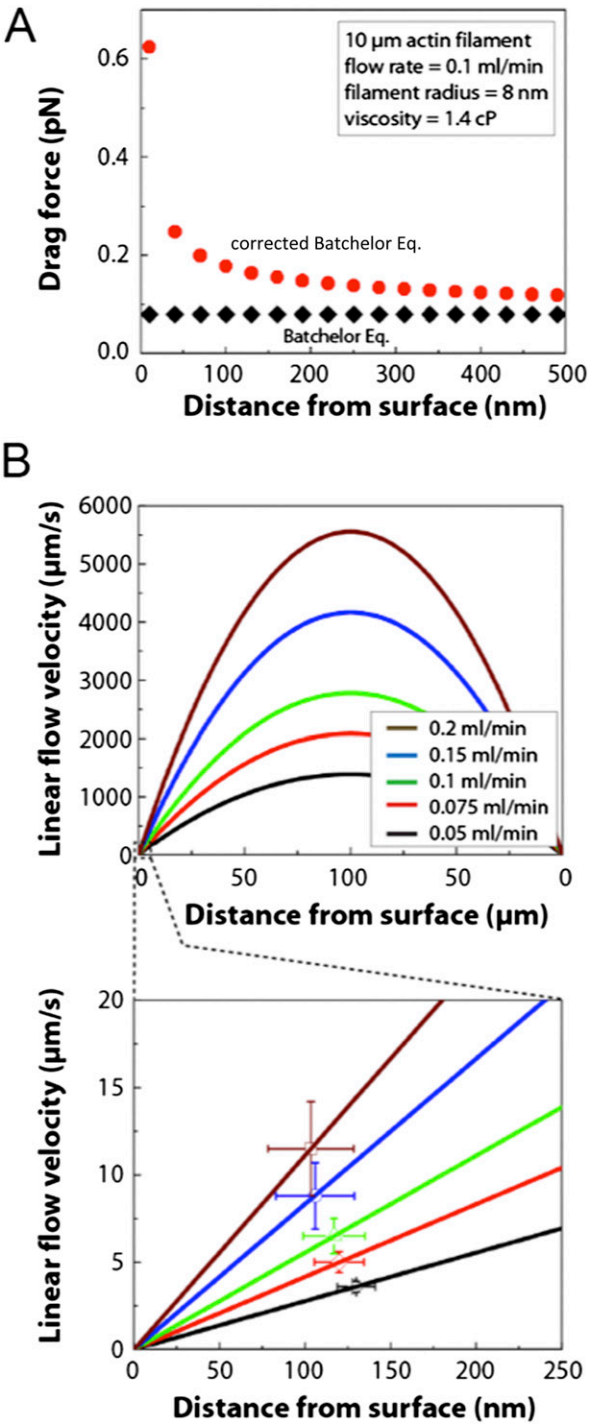

Fig. S1. Impact of surface proximity on surface-tethered filaments. (*A*) Force estimates for a tethered actin filament. Black diamonds: estimated force calculated from the Batchelor formula with no correction for filament height from the surface (1). Red circles: estimated force-corrected effects due to surface proximity over a range of distances from the surface. (*Inset*) List of the relevant parameters (bulk flow rate, filament radius, and solution viscosity). Representative calculations are shown for a 10-μm actin filament, approximately the average length of the filaments observed in this study. These calculations illustrate that proximity to the surface has a substantial effect on the force on filaments, but this effect diminishes rapidly with distance from the surface and is less than threefold for filaments located >50 nm from the surface. (*B*) Flow velocity profiles for (*Upper*) the entire cross-section of the chamber and (*Lower*) the region close to the surface. Colored lines indicate the calculated flow velocity profile as a function of distance from the surface at different bulk flow rates, as

Legend continued on following page

indicated (*Inset*). The linear flow velocities in the imaging plane were measured by tracking filaments broken from anchored filaments (Table S2), and these data were superimposed on the flow velocity profiles to estimate the positions of the filaments relative to the surface. The open circles indicate mean velocities of broken filaments plotted on the flow velocity profiles for each different flow rate; vertical and horizontal error bars correspond to SEM on the flow measurements and corresponding height calculations, respectively, based on the experimentally measured linear flow velocities. At all bulk flow rates, the velocities of broken filaments correspond to the flow rate at ~100–130 nm from the surface.

1. Batchelor GK (1970) Slender-body theory for particles of arbitrary cross-section in Stokes flow. *Journal of Fluid Mechanics* 44:419–440.

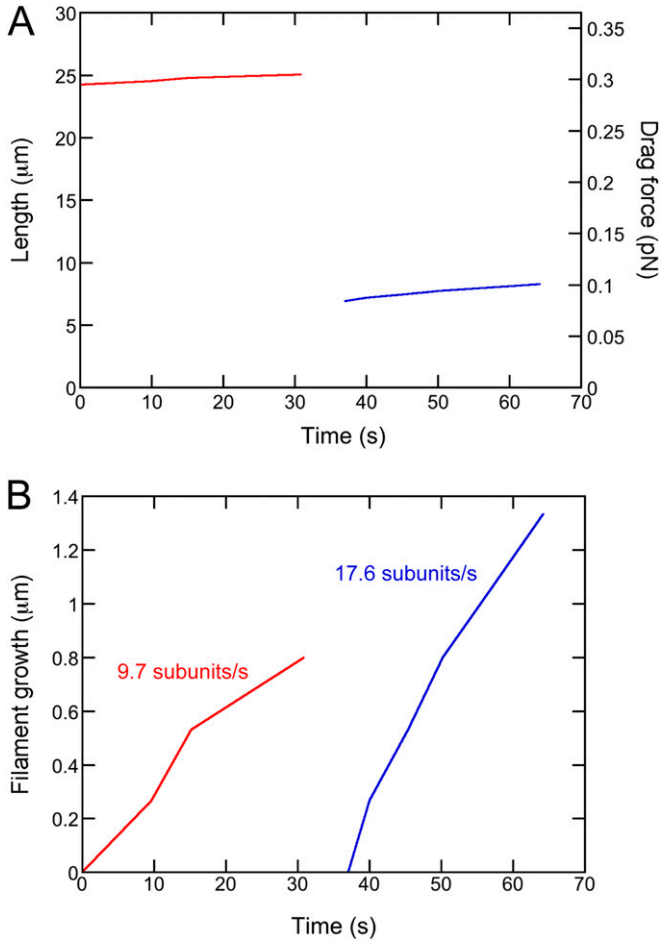

Fig. S2. Filament elongation before and after spontaneous filament breakage. Buffer conditions: 1.5 μM actin (33% Oregon Green-actin) in microscopy buffer with 0.25% methylcellulose (15 centipoise at 2%). Barrier height was 25 nm. (*A*) Evolution of the length of a single filament in the absence of profilin with a bulk flow of 0.05 mL/min. The red line corresponds to elongation that occurs before a spontaneous breakage event and the blue line corresponds to elongation that occurs following the breakage event. The estimated hydrodynamic force applied to the filament is shown on the right axis and is proportional to the length of the filament. (*B*) Filament growth before (red line) and after (blue line) the filament breakage event depicted in *A*. The filament break instantaneously decreases the drag force (seen in *A*) and produces an increase in the polymerization rate.

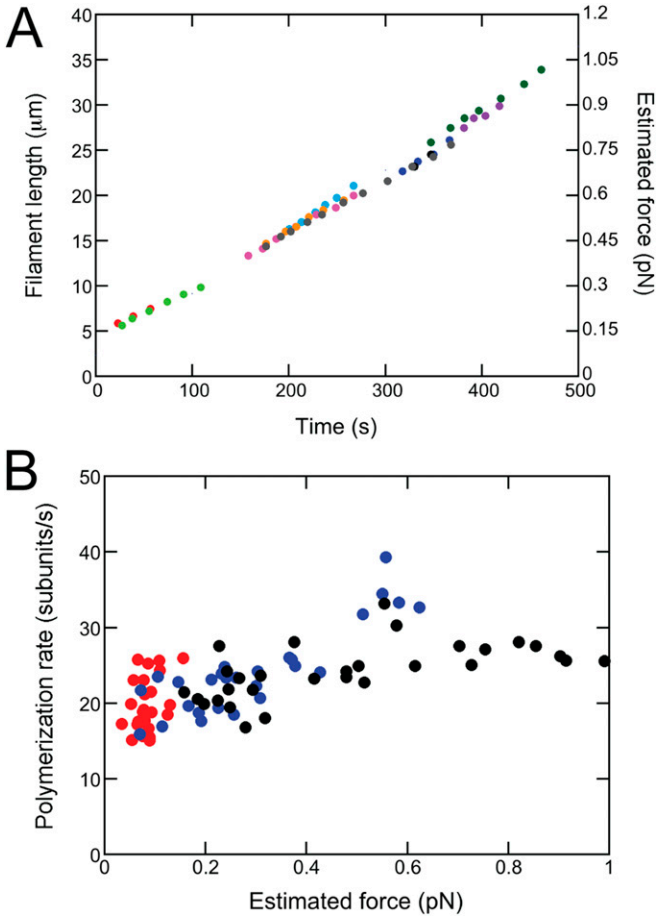

Fig. S3. Effect of tension on formin-mediated polymerization in the presence of 5 μM profilin. Buffer conditions: 1.5 μM actin (33% Oregon Green-actin) with 5 μM profilin in microscopy buffer with 0.25% methylcellulose (15 cP at 2%). Barrier height was 25 nm. (*A*) Collection of elongation trajectories of filaments in the presence of 0.2 mL/min bulk flow, aligned by length. Each filament is represented by a different color and, for clarity, every third data point is shown. (*B*) Dependence of polymerization rates on the drag force exerted on filaments at 0.05 (red circles), 0.1 (blue circles), and 0.2 (black circles) mL/min bulk flow. Polymerization rates and drag forces (calculated according to Eq. **3**) were measured at various intervals over the course of the elongation experiment.

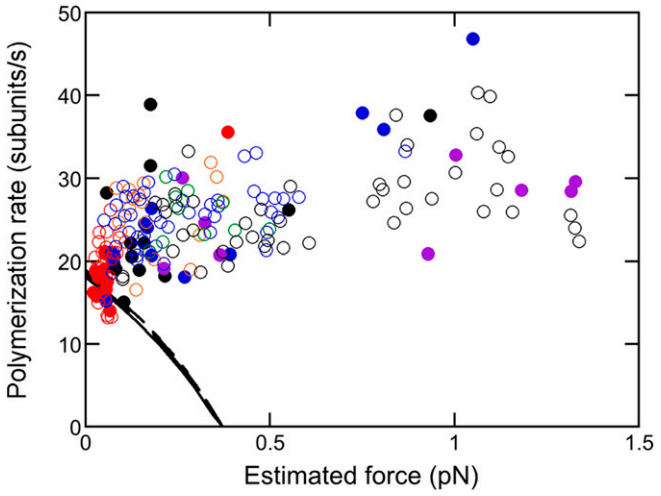

Fig. S4. Comparison of experimental and simulated polymerization rates in the presence of 2.5 μM profilin. Experimental data: The points show the dependence of measured polymerization rates on the drag force exerted on each filament at bulk flow rates of 0.05 (red circles), 0.075 (orange circles), 0.1 (blue circles), 0.15 (green circles), 0.2 (black circles), and 0.5 (purple circles) mL/min. Data were collected using 10-nm barriers (filled circles) and 25-nm barriers (open circles). Simulations: Lines show the dependence of simulated polymerization rates on drag force using a gating factor that declines linearly from 0.75 without force to 0 at forces >0.3 pN. Table S3 lists rate constants for the formation of intermediate species [formin homology (FH)1–profilin, FH1–profilin–actin, FH1–profilin–actin–barbed end, barbed end–profilin, and filamentous actin]. The simulations used four different FH1 loop closure rates: solid line: 5,000 s^{-1} that reproduces the polymerization rates of filaments associated with wild-type Bni1(FH1FH2)p in the absence of force; long dashes: 25 times faster than wild-type; short dashes: 125 times faster; dotted line: 625 times faster.

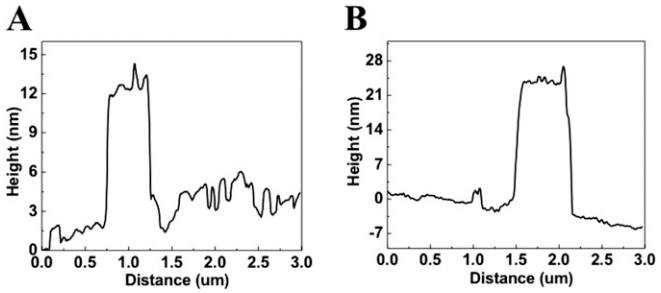

Fig. S5. Height profiles of chromium barriers on fused-silica slides. (*A*) Ten-nanometer and (*B*) 25-nm barriers were scanned by atomic force microscopy in tapping mode at a 1-Hz scanning rate.

Table S1. Summary of Bni1(FH1FH2)p-mediated polymerization rates

	Flow rate, mL/min						
Profilin, μM	0.0	0.05	0.075	0.1	0.15	0.2	0.5
0	13.6 ± 1.6*	13.3 ± 0.9	12.7 ± 2.0	10.8 ± 1.5	10.8 ± 0.7	4.4 ± 0.6	2.3 ± 0.2
1		17.1 ± 1.9	18.1 ± 0.6	20.9 ± 2.3	20.0 ± 1.9	20.2 ± 2.0	
2.5		20.5 ± 1.6	21.3 ± 2.6	25.2 ± 1.6	25.3 ± 3.8	25.8 ± 2.6	
5		19.2 ± 2.2	19.2 ± 2.4	20.1 ± 1.7	19.9 ± 2.4	20.9 ± 1.8	
10		12.5 ± 3.1	14.8 ± 1.9	15.6 ± 1.3	15.3 ± 1.6	15.4 ± 1.7	

*Polymerization rates are in subunits per second. This rate was measured on a myosin-coated slide surface, as described (1). Errors are SEM from the analysis of 10–30 filaments.

1. Kuhn JR, Pollard TD (2005) Real-time measurements of actin filament polymerization by total internal reflection fluorescence microscopy. *Biophys J* 88(2):1387–1402.

Table S2. Summary of flow rates and drag force imposed at each bulk flow rate

Bulk flow rate, mL/min	Linear flow rate,* μm/s	Drag force per μm filament,† pN	Height from the surface,‡ nm
0.05	3.6 ± 0.3	0.009 ± 0.001	130.0 ± 11.0
0.075	5.0 ± 0.6	0.013 ± 0.0015	120.0 ± 14.5
0.10	6.5 ± 1.0	0.017 ± 0.0024	117.0 ± 18.0
0.15	8.8 ± 1.9	0.024 ± 0.0046	106.0 ± 23.0
0.20	11.2 ± 2.7	0.030 ± 0.0066	103.5 ± 25.0

*Flow rates within the observation plane were measured by tracking the trajectories of broken actin filaments that passed through the observation volume. Errors are SEMs from the analysis of 10 broken filaments.
†Drag force per micron of filament was estimated from a height-corrected form of the Batchelor equation.
‡The height of the filaments from the surface was estimated by comparing the linear flow rates with the calculated flow velocity profiles (Fig. S1*B*).

Table S3. Rate constants used in the model of FH1FH2-mediated polymerization

FH1-independent actin subunit addition		
FH2 domain conformational changes		
	Gating factor*	$k_o/(k_o + k_c)$
	k_o	(1,000 × gating factor) s^{-1}
	k_c	(1,000 − k_o) s^{-1}
Actin binding to FH2-bound barbed end		
	k_A^{B+}	11.6 $\mu M^{-1}\cdot s^{-1\dagger}$
	k_A^{B-}	1.4 $s^{-1\dagger}$
Profilin–actin binding to FH2-bound barbed end		
	k_{PA}^{B+}	10 $\mu M^{-1}\cdot s^{-1\ddagger}$
	k_{PA}^{B-}	140 s^{-1} (DB)
Profilin binding to FH2-bound barbed end		
	k_P^{B+}	10 $\mu M^{-1}\cdot s^{-1\ddagger}$
	k_P^{B-}	2,500 $s^{-1\ddagger}$
Assembly of profilin–actin onto the FH1 domain		
Profilin–actin binding to FH1 domain§		
	k_{PA}^{F+}	7 $\mu M^{-1}\cdot s^{-1\P}$
	k_{PA}^{F-}	140 s^{-1} (DB)
Profilin binding to FH1 domain§		
	k_P^{F+}	200 $\mu M^{-1}\cdot s^{-1\|\|}$
	k_P^{F-}	4,000 $s^{-1\ddagger}$
Actin binding to FH1-bound profiling		
	k_A^{F+}	20 $\mu M^{-1}\cdot s^{-1}$**
	k_A^{F-}	30 $s^{-1\dagger\dagger}$
FH1 domain loop closure		
Closure of FH1 domain loop		
	r_F^+	6.25×10^4 $s^{-1\S\S}$
	r_F^-	1.25×10^6 s^{-1} (DB)
Closure of profilin-bound FH1 domain loop		
	r_{PF}^+	5,000 $s^{-1\P\P}$
	r_{PF}^-	1.25×10^6 $s^{-1\S\S}$
Closure of profilin–actin–bound FH1 domain loop		
	r_{PAF}^+	5,000 $s^{-1\P\P}$
	r_{PAF}^-	50,000 s^{-1} (DB)

o, open conformation; c, closed conformation; A, actin; P, profilin; B, barbed end; PA, profilin-actin; F, FH1 domain; PF, profilin-bound FH1 domain; PAF; profilin-actin-bound FH1 domain. DB, rate constants determined from detailed balance calculations, as described (1, 2).

*The gating factor is the fraction of time that the barbed end-bound FH2 domain remains in the open, actin binding-competent conformation without profilin.

†From measurements of elongation of free barbed ends with purified ATP-actin monomers (3).

‡From Vavylonis et al. (2).

§These rate constants were varied to produce the trends in Fig. 4 *C* and S4.

¶This value was optimized to fit the experimental data as in Paul and Pollard (1).

||Measured rate of bovine spleen profilin binding to polyproline (4).

**From Paul and Pollard (1). To account for the reduced mobility of profilin when bound to the FH1 domain, this value is smaller than the experimentally measured association rate constant for profilin to actin.

††This rate is the product of the K_d for profilin–actin and the profilin–actin association rate. Although the K_d for *Saccharomyces cerevisiae* profilin and skeletal muscle actin has been experimentally measured to be 3 μM, we found that a K_d of 1.5 μM best fit our experimental data.

§§From Paul and Pollard (1), assuming that loop closure is faster for unbound FH1 than for profilin- or profilin–actin–bound FH1, and that profilin binding to FH1 does not affect the affinity of profilin for the barbed end.

¶¶This value was varied to fit experimental data, as in Paul and Pollard (1).

1. Paul AS Pollard TD (2009) Energetic requirements for processive elongation of actin filaments by FH1FH2-formins. *J Biol Chem* 284(18):12533–12540.
2. Vavylonis D, Kovar DR, O'Shaughnessy B, Pollard TD (2006) Model of formin-associated actin filament elongation. *Mol Cell* 21(4):455–466.
3. Pollard TD (1986) Rate constants for the reactions of ATP- and ADP-actin with the ends of actin filaments. *J Cell Biol* 103(6 Pt 2):2747–2754.
4. Perelroizen I, Marchand JB, Blanchoin L, Didry D, Carlier MF (1994) Interaction of profilin with G-actin and poly(L-proline). *Biochemistry* 33(28):8472–8478.

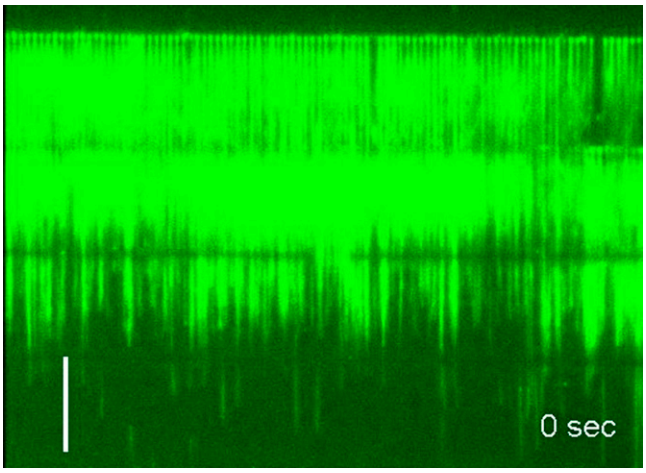

Movie S1. Lipid-tethered, formin-bound actin filaments extend upon introduction of buffer flow. Buffer conditions: 1.5 μM actin (33% Oregon Green-actin) in microscopy buffer (10 mM imidazole, pH 7.0, 50 mM KCl, 1 mM $MgCl_2$, 1 mM EGTA, 50 mM DTT, 0.2 mM ATP, 0.02 mM $CaCl_2$, 15 mM glucose, 0.02 mg/mL catalase, 0.1 mg/mL glucose oxidase). Movie of formin-bound actin curtains assembled at four barriers on the lipid-coated surface of a microfluidic chamber. Flow is introduced into the chamber and transiently paused. (Scale bar, 20 μm.) The elapsed time is indicated.

Movie S1